Ecological Processes

RESEARCH

Open Access

Physiological responses and algae inhibition of *Pontederia cordata* to simulated eutrophication and acid rain co-pollution

Yan Li[1†], Xi Qi[1†], Jianpan Xin[1], Chu Zhao[1] and Runan Tian[1*]

Abstract

Background Eutrophication and acid rain are two threats that many water bodies must contend with. Eutrophication and climate change have accelerated widespread outbreaks of cyanobacterial blooms as both have become more severe. *Pontederia cordata*, a garden ornamental plant, can inhibit some algae growth and remove total nitrogen (TN) and total phosphorus (TP) from the water. In this study, we investigated how simulated acid rain and eutrophication co-pollution affected *P. cordata*'s growth physiology and ability to inhibit algae growth.

Results Under mild eutrophication (2 mg·L^{-1} TN, 0.4 mg·L^{-1} TP, and 15 mg·L^{-1} COD_{Mn}) or weak acid rain (pH = 5.0), *P. cordata* alleviated the degree of cell membrane lipid peroxidation by stabilizing superoxide dismutase (SOD) and catalase (CAT) activities in the leaves, allowing for normal plant growth. Under mild eutrophication and acid rain conditions, cultured *P. cordata* water samples maintained strong algae inhibition by reducing the Chl *a* content and SOD activity of *Microcystis aeruginosa* cells. Compound stress where acid rain was the primary inhibitory factor along with moderate or severe eutrophication inhibited *P. cordata* growth, which probably reduced the input of algae-inhibiting allelochemicals, thus reducing its ability to inhibit algae.

Conclusions In summary, *P. cordata* has application potential in mild eutrophic water and acid rain (pH ≥ 4). These findings provide guidance for further research on phytoremediation and algae control in scenarios of compound pollution.

Keywords *Pontederia cordata*, *Microcystis aeruginosa*, Eutrophication, Acid rain, pH, Physiological response

Introduction

One of the top three ecological and environmental issues facing the planet today is acid rain. Known as wet deposition, it refers to rain, snow, fog, hail, or any other type of atmospheric precipitation with a pH of less than 5.6. Strong acid rain has a pH of less than 4.5, while weak acid rain ranges from 4.5 to 5.6. China is the third largest acid rain area in the world after Europe and North America, with 40% of its territory polluted by acid rain. China's estimated annual economic losses caused by acid rain pollution are as high as 110 billion yuan. In 2016, the SO_2 emissions of India exceeded those of China. Up until 2030, SO_2 and NO_x emissions, which are India's primary contributors to acid deposition, are anticipated to rise (Andrade et al. 2020). Acid rain damages plants mainly through toxic effects on aboveground morphological structures, mineral element metabolism, antioxidant system, and photosynthesis. Andrade et al. (2020) found that simulated acid rain (SAR) (pH = 4.5) altered epidermal relief and resulted in the wilting of epidermal cells of *Joannesia princeps*. Verónica et al. (2020) examined the effects of SAR on *Liquidambar styraciflua* and *Fraxinus*

†Yan Li and Xi Qi contributed equally to this research.

*Correspondence:
Runan Tian
tianrunan@njfu.edu.cn
[1] College of Landscape Architecture, Nanjing Forestry University, Nanjing 210037, Jiangsu, China

uhde, the two most prevalent urban trees in Mexico City, and discovered that SAR (pH = 2.5) reduced the chlorophyll content in the leaves, altered cuticle scaling, and impacted the formation of epicuticular wax aggregates. In the leaves of two varieties of tomato, Debnath et al. (2018) showed that the contents of chlorophyll, carotenoid, total soluble protein, and soluble sugar decreased as the pH of SAR decreased, while the contents of hydrogen peroxide and lipid peroxide increased. Specifically, enzymatic and non-enzymatic antioxidants (total phenols, total flavonoids, and iron reduction) decreased at a pH of 2.5. The harmful effects of acid rain on plants are also reflected in its superposition with other pollutants. Academics from around the world are paying more attention to research on the combined stress of acid rain and other environmental factors (Du et al. 2022; Neves et al. 2009).

A significant amount of nitrogen and phosphorus nutrients have accumulated in rivers and lakes due to the increased discharge of domestic, industrial, and agricultural wastewater. That has led to an excess of nitrogen and phosphorus nutrients and a decline in the quality of the water. Eutrophication has become a focus of global water environmental governance and research. Additionally, eutrophication and climate change have catalyzed the expansion of cyanobacterial blooms in aquatic ecosystems worldwide (Huisman et al. 2018). In the 1980s, the scale of cyanobacterial blooms was 68% in 71 large lakes (each with an area of > 100 km^2), which has continued to grow (Ho et al. 2019). The frequent occurrence of cyanobacteria blooms and the ongoing buildup of algal toxins threaten organismal and human health through the food chain, disrupt the functioning of aquatic ecosystems, and destroy the ecological balance of the water environment (D'Anglada 2021; Lee et al. 2017). Specifically, *Microcystis aeruginosa* is a common dominant species of cyanobacterial blooms in many eutrophic lakes (Princiotta et al. 2019). How to effectively control or eliminate the spread of algae is of great importance. Many physical and chemical algae suppression methods have been implemented, such as artificial mixing (Visser et al. 2016), ultrasound treatment (Kong et al. 2019), UV-activated persulfate (Wang et al. 2016a), and flocculants use (Wang et al. 2018). However, although these methods remove algae in the short term, they are expensive and cause secondary pollution. Mjelde and Faafeng (1997) found higher biomass densities of aquatic plants in 24 lakes in Norway, where lower phytoplankton densities led to better water quality. Indeed, aquatic macrophytes release allelochemicals via root secretion, leaching, volatilization, and the decomposition of plant residues in the water, which is an effective strategy for preventing algae development (Hilt and Gross 2008). Recently, macrophyte allelochemicals have attracted attention as substitutes for synthetic chemicals in cyanobacterial harmful algal bloom (CyanoHAB) control due to their environmental safety and higher biodegradability (Tazart et al. 2021). The inhibition of allelochemicals released by aquatic plants on the physiological metabolism, growth, and development of algae is mainly reflected in the following three aspects: (1) reduced chlorophyll content of algae cells and blocked photosynthetic electron transmission, which weakens the photosynthetic capacity and inhibits photosynthesis (especially photosystem II); (2) inhibited activities of antioxidant enzymes and adenosine triphosphate (ATP) in algal cells, which induce oxidative damage to algal cells and hinder their absorption of calcium, magnesium, and other mineral elements; and (3) increased destruction of the permeability of the cell membrane, which results in the exudation and loss of cell contents and even leads to programmed cell death (Wang et al. 2016b). Moreover, differences in the nutrient and pH levels exert important effects on plant allelopathy (Allen et al. 2017). According to the growth–differentiation balance hypothesis (GDBH), plants will decrease the input of allelochemicals as stress increases and their physiological functions are severely compromised, which will weaken allelopathy (Bauer et al. 2010).

Pontederia cordata belongs to the Pontederiaceae family and is a perennial emergent plant. Due to its developed roots, large biomass, appealing flowers, and long flowering period, this plant has high garden ornamental value. Additionally, this plant lowers the levels of total nitrogen (TN) and total phosphorus (TP) in eutrophic water, and its organic acid allelochemicals (succinic acid, cinnamic acid, and vanillic acid) have some effects that inhibit the growth of algae. It has a good application potential in the treatment of urban sewage (Qian et al. 2019; Tian et al. 2011). However, when faced with the dual stress of eutrophication and acid rain, the physiological response of *P. cordata* and corresponding effects on algae inhibition remain unknown. Thus, this study aimed to address the following research objectives: (1) to determine the effects of the compound stress of eutrophication and acid rain on the growth and photosynthetic capacity of *P. cordata* using the relative growth rate (RGR), root activity, and total chlorophyll (Chl *T*) content in the leaves; (2) to investigate the degree of membrane peroxidation and antioxidant responses under compound stress through estimating the relative conductivity (REC), malondialdehyde (MDA) content, and superoxide dismutase (SOD) and catalase (CAT) activities in the leaves; and (3) to elucidate the effects of various cultured water samples of *P. cordata* under different simulated eutrophication and acid rain treatments on the growth and physiological metabolism of *M. aeruginosa* by measuring the SOD activity, MDA content, and chlorophyll content of *M.*

aeruginosa cells and the inhibition rates on algae. These results will provide a theoretical basis for future studies on phytoremediation and algae control under eutrophication and acid rain co-pollution.

Materials and methods

Location and plant materials

The present study was conducted in a greenhouse at the National Landscape Architecture Experimental Teaching Demonstration Center, Nanjing Forestry University, Nanjing, China (118° 49′ E, 32° 04′ N). *P. cordata* seedlings with a similar number of leaves and of the same height were selected for experimentation, and then planted in Hoagland nutrient solution. *M. aeruginosa* was purchased from the Institute of Hydrobiology, Chinese Academy of Sciences (Wuhan, China), and then amplified and cultured in BG-11 medium. The culture conditions were 25 ± 2 °C, 3000 lx light, and a 12/12 h photoperiod. After the logarithmic growth period, the experiment began.

Eutrophication of water samples

The eutrophication of tested water samples prepared from $C_6H_{12}O_6$, $CO(NH_2)_2$, and KH_2PO_4 was set at four levels (E0, E1, E2, and E3) (Table 1). E0 was the control group. The TN and TP contents and the permanganate index (COD_{Mn}) of E0 were referred to the III water quality standard of GB3838-2002 (Ministry of Environmental Protection of the People's Republic of China 2002), which applies to centralized domestic drinking water. The TN, TP, and COD_{Mn} of E1 referred to the V-grade water quality standard, which applies to agricultural and general landscape water. In the E2, the TN and the TP were both 5 times of the V water quality standard; in the E3, the TN and the TP were both 10 times.

SAR preparation and application

The average annual pH of precipitation in the Yangtze River Delta of China is 4.87 ± 0.28 (Li et al. 2021). The SO_4^{2-}/NO_3^- ranges between 2.4 and 2.9 (Chen 2018). To simulate acid rain, analytical pure H_2SO_4 and HNO_3 were applied to prepare acid rain mother liquor (pH = 1.0) with an SO_4^{2-}/NO_3^- volume ratio of 3:1. Then, the pH of acid rain mother liquor was diluted to 4.0 and 5.0. Ultrapure water (pH = 7.0) was used for the control group.

Experimental design

Plants exposed to eutrophication and SAR spraying

The experiment was arranged in a factorial scheme that was completely randomized using two factors (eutrophication and pH), four eutrophication levels (E0, E1, E2, and E3), and three pH levels (7.0, 5.0, and 4.0) (Table 2). Three replicates from each of the 12 treatments were used, yielding a total of 36 experimental units. Plants with good growth and a biomass value of 80 g in Hoagland nutrient solution were selected, washed, and cultured in plastic buckets containing 1.5 L eutrophic water. Throughout the experiment, water samples were changed every 7 d. After two weeks, the plants were sprayed four times every 7 d with SAR or ultrapure water (10 mL per plant). The day of foliar spraying was regarded as day 1. During foliar spraying, the plastic buckets were completely covered with plastic film to prevent SAR spraying from affecting the pH of water samples. After 28 d, the cultured water samples were harvested for the *M. aeruginosa* inoculation test.

Algae inoculated in cultured water of plants exposed to eutrophication and sprayed with SAR

M. aeruginosa got exposed to different cultured water samples of plants mentioned above. The cultured water samples were filtered with medium-speed filter paper and a 0.45-μm microporous membrane to filter out protozoa and microorganisms. E0 + pH 7.0 was used as the control group. The initial OD_{650} value of algae was 0.1. The day of inoculation was regarded as day 0, and the processing time lasted for 7 d. The algal density was measured on day 1, and algal cells were harvested for physiological index determination on days 1, 3, 5, and 7.

Table 1 Different elements' concentrations in tested water samples at various eutrophication levels

Eutrophication	Elements		
	TN ($mg \cdot L^{-1}$)	TP ($mg \cdot L^{-1}$)	COD_{Mn} ($mg \cdot L^{-1}$)
E0	1	0.2	6
E1	2	0.4	15
E2	10	2.0	24
E3	20	4.0	36

Table 2 Compound treatments of simulated acid rain (SAR) and eutrophication on *Pontederia cordata*

Simulated eutrophication	SAR		
	pH = 7.0	pH = 5.0	pH = 4.0
E0	E0 + pH 7.0	E0 + pH 5.0	E0 + pH 4.0
E1	E1 + pH 7.0	E1 + pH 5.0	E1 + pH 4.0
E2	E2 + pH 7.0	E2 + pH 5.0	E2 + pH 4.0
E3	E3 + pH 7.0	E3 + pH 5.0	E3 + pH 4.0

Measurement of indices

Related indicators of P. cordata

Determination of RGR: Plants were harvested on days 1 and 28, washed with ultrapure water, dried with filter paper, and weighed with an electronic balance. The RGR was calculated using the following equation: $RGR = (W_1 - W_0)/W_0 \times 100\%$, where W_1 is the initial fresh weight, and W_0 is the final fresh weight.

Root activity (Wang 2006): Fresh plant roots (0.3 g) were harvested on day 28 and then soaked in a mixture containing 0.4% 2,3,5-triphenyltetrazolium chloride (TTC) and phosphate buffer (1/15 M, pH = 7.0) for 1 h at 37 °C under continuous darkness. Afterward, 2 mL of 1 M sulfuric acid was added to terminate the reaction. Then, ethyl acetate and a small amount of quartz sand were added to the root samples. After grinding, the OD_{485} of the red extract was measured to calculate the reduction strength of tetrazolium.

On days 7, 14, 21, and 28, the Chl *T* and MDA contents, SOD and CAT activities, and REC of *P. cordata* leaves were calculated following previously described methods (Wang 2006).

Chl *T* content: Leaves (0.1 g) were soaked in 10 mL of 95% ethanol at room temperature under continuous darkness for 24 h until the leaves were completely white. Afterward, the OD_{649} and OD_{665} of the supernatant were recorded using an ultraviolet–visible spectrophotometer (Lambda 25, Perkin-Elmer, Waltham, MA, USA).

SOD activity: Leaves (0.3 g) were soaked in 6 mL of phosphate buffer (0.05 M, pH = 7.8), then ground to a homogenate, and centrifuged at 4000 $r \cdot min^{-1}$ for 10 min. The reaction system was exposed to 4000 lx light for 20 min, and the absorbance was measured at 560 nm.

CAT activity: The extraction method of the enzyme solution was the same regarding SOD. The reaction system was preheated to 25 °C. Then, 0.3 mL of 0.1 M H_2O_2 was added to the system, and the OD_{240} was determined. Readings were recorded every minute for 3 min.

REC: The cell membrane permeability was measured using a conductometer. After the main vein and margin of leaves were removed, the leaves were punched into disks with a diameter of 6 mm. The leaf disks were soaked in 15 mL of distilled water with a conductivity (R_0) of 0 at room temperature for 24 h. Then, the conductivity (R_1) was measured with a conductivity meter (DDS-307 type, Inesa, Shanghai, China). Afterward, the disks were heated in a boiling water bath for 15 min; then the conductivity (R_2) was measured at a constant temperature (20–25 °C).

MDA content: A total of 2 mL of supernatant and 2 mL of 0.67% thiobarbituric acid (TBA) were mixed and boiled for 20 min. After quickly cooling, the mixture was centrifuged at 4000 $r \cdot min^{-1}$ for 10 min. The absorbance was measured at 450, 532, and 600 nm.

Related indicators of M. aeruginosa

Determination of inhibition rates (IR) on algal infrared: BG-11 medium mixed with water samples in corresponding degrees was used as the control. The OD_{650} was measured, as it reflects the algae density. The IR was calculated using the following equation: $IR = (1 - N_1/N_0) \times 100\%$, where N_1 and N_0 are the algae densities of the treatment and control groups, respectively.

The Chl *a* content in *M. aeruginosa* cells was measured using the hot ethanol method (Chen et al. 2006). First, microporous filter membranes enriched with algal cells were sheared, and then 8 mL of 90% hot ethanol solution was quickly added for extraction at 80 °C. After 2 min, the mixtures were immediately transferred to an ultrasonic cleaner and crushed in a 50-Hz ice bath for 40 min. After static extraction in the dark for 2 h, the mixtures were centrifuged at 4 °C and 5000 $r \cdot min^{-1}$ for 12 min. The supernatant was added to 2 mL of 90% ethanol and centrifuged again. The absorbance was measured at 665 and 750 nm.

The SOD activity in algal cells was quantified using nitrogen blue tetrazole (NBT) colorimetry (Gao 2006). First, 10 mL of algal cell solution was centrifuged at 4 °C and 9000 $r \cdot min^{-1}$ for 15 min. The supernatant was poured out, and 5 mL of buffer solution (0.05 M, pH = 7.8) was added. Then, the mixture was placed in an ultrasonic cleaner and crushed in a 50-Hz ice bath for 40 min. After centrifugation for 15 min, the reaction system was exposed to strong light for 20 min, and the absorbance was determined at 560 nm.

The MDA content in algal cells was measured using the TBA method (Wu and Ye 2016). First, 1 mL of supernatant and 2 mL of TBA solution were mixed and heated in a boiling water bath for 20 min. After cooling, the mixture was centrifuged at 4000 $r \cdot min^{-1}$ for 10 min. Then, the OD_{450}, OD_{532}, and OD_{600} of the supernatant were measured.

Data analysis

The data were analyzed using SPSS v26.0 software. Tukey's test was used for multiple comparisons based on significant differences detected by the analysis of variance (ANOVA). Graphs were prepared using DataGraph v4.7.1 and Adobe Illustrator 2019.

Results

Growth and physiological responses of *P. cordata* to simulated eutrophication and acid rain

Relative growth rate (RGR)

Significant differences were detected in the RGR of *P. cordata* under different main effects of simulated eutrophication (Table 3). Compared to the control, no significant differences were detected in the RGR of *P. cordata* with

Table 3 The variance analysis of the RGR, root activity, Chl *T* content, SOD activity, CAT activity, REC, and MDA content of *P. cordata* under the simulated acid rain spraying times, simulated acid rain (SAR) and simulated eutrophication

Indicators	Source	Type III sum of squares	*df*	Mean square	*F*	Sig.
RGR (%)	Modified model	9333.150	11	848.468	12.879	< 0.05
	SAR	2189.120	2	1094.560	16.615	< 0.05
	Eutrophication	5282.438	3	1760.813	26.728	< 0.05
	SAR × eutrophication	1861.592	6	310.265	4.710	< 0.05
	Error	1581.106	24	65.879		
	Total	10,914.255	35			
Root activity ($\mu g \cdot g^{-1} \cdot h^{-1}$)	Modified model	352.927	11	32.084	807.998	< 0.05
	SAR	98.645	2	49.323	1242.123	< 0.05
	Eutrophication	133.333	3	44.444	1119.271	< 0.05
	SAR × eutrophication	120.948	6	20.158	507.653	< 0.05
	Error	0.953	24	0.040		
	Total	353.879	35			
Chl *T* content ($mg \cdot g^{-1}$)	Modified model	74,306,691.659	47	1,580,993.440	72.569	< 0.05
	Spraying time	43,701,031.990	3	14,567,010.660	668.640	< 0.05
	SAR	8,536,639.803	2	4,268,319.902	195.920	< 0.05
	Eutrophication	7,771,249.193	3	2,590,416.398	118.903	< 0.05
	Spraying time × SAR	936,064.140	6	156,010.690	7.161	< 0.05
	Spraying time × eutrophication	7,071,024.968	9	785,669.441	36.063	< 0.05
	SAR × eutrophication	2,580,471.667	6	430,078.611	19.741	< 0.05
	Spraying time × SAR × eutrophication	3,710,209.899	18	206,122.772	9.461	< 0.05
	Error	2,091,459.343	96	21,786.035		
	Total	76,398,151.002	143			
SOD activity ($U \cdot g^{-1}$)	Modified model	14,410.544	47	306.607	204.383	
	Spraying time	9056.557	3	3018.852	2012.351	< 0.05
	SAR	529.412	2	264.706	176.451	< 0.05
	Eutrophication	570.129	3	190.043	126.682	< 0.05
	Spraying time × SAR	624.470	6	104.078	69.378	< 0.05
	Spraying time × eutrophication	668.070	9	74.230	49.481	< 0.05
	SAR × eutrophication	706.253	6	117.709	78.464	< 0.05
	Spraying time × SAR × eutrophication	2255.654	18	125.314	83.534	< 0.05
	Error	144.016	96	1.500		
	Total	14,554.560	143			
CAT activity ($U \cdot g^{-1} \cdot min^{-1}$)	Modified model	48,394,887.489	47	1,029,678.457	138.113	< 0.05
	Spraying time	34,115,828.370	3	11,371,942.790	1525.343	< 0.05
	SAR	1,986,408.073	2	993,204.036	133.221	< 0.05
	Eutrophication	3,350,353.184	3	1,116,784.395	149.797	< 0.05
	Spraying time × SAR	1,570,254.211	6	261,709.035	35.104	< 0.05
	Spraying time × eutrophication	5,552,955.866	9	616,995.096	82.759	< 0.05
	SAR × eutrophication	304,539.296	6	50,756.549	6.808	< 0.05
	Spraying time × SAR × eutrophication	1,514,548.493	18	84,141.583	11.286	< 0.05
	Error	715,712.233	96	7455.336		
	Total	49,110,599.720	143			

Table 3 (continued)

Indicators	Source	Type III sum of squares	*df*	Mean square	*F*	Sig.
REC (%)	Modified model	39,799.495	47	846.798	291.970	
	Spraying time	21,763.019	3	7254.340	2501.250	< 0.05
	SAR	2892.592	2	1446.296	498.674	< 0.05
	Eutrophication	7238.790	3	2412.930	831.963	< 0.05
	Spraying time × SAR	965.229	6	160.872	55.467	< 0.05
	Spraying time × eutrophication	2038.650	9	226.517	78.101	< 0.05
	SAR × eutrophication	1150.834	6	191.806	66.133	< 0.05
	Spraying time × SAR × eutrophication	3750.381	18	208.354	71.839	< 0.05
	Error	278.427	96	2.900		
	Total	40,077.922	143			
MDA content ($nmol·g^{-1}$)	Modified model	4963.725	47	105.611	225.012	< 0.05
	Spraying time	1186.218	3	395.406	842.441	< 0.05
	SAR	1493.204	2	746.602	1590.689	< 0.05
	Eutrophication	1625.039	3	541.680	1154.087	< 0.05
	spraying time × SAR	63.515	6	10.586	22.554	< 0.05
	Spraying time × eutrophication	64.575	9	7.175	15.287	< 0.05
	SAR × eutrophication	410.638	6	68.440	145.816	< 0.05
	Spraying time × SAR × eutrophication	120.536	18	6.696	14.267	< 0.05
	Error	45.058	96	0.469		
	Total	5008.783	143			

Differences in the seven indicators following interactive effects of four spraying times, four eutrophication levels (E0, E1, E2, and E3) and three pH levels (7.0, 5.0, and 4.0) were analyzed using a general linear model (GLM), with spraying time, eutrophication, and pH as fixed factors, and the RGR, root activity, or Chl *T*, or SOD, or CAT, or REC, or MDA as a dependent variable (Additional file 1)

Table 4 The main effects of simulated acid rain spraying times, simulated eutrophication, or simulated acid rain (SAR) on *Pontederia cordata*

Main effects		Index						
		RGR (%)	Root activity ($μg·g^{-1}·h^{-1}$)	Chl *T* ($mg·g^{-1}$)	SOD ($U·g^{-1}$)	CAT ($U·g^{-1}·min^{-1}$)	REC (%)	MDA ($nmol·g^{-1}$)
Simulated acid rain spraying times	1	–	–	1862.03 ± 78.62^{b}	57.35 ± 1.42^{d}	395.71 ± 8.06^{d}	19.76 ± 1.23^{c}	11.51 ± 0.76^{c}
	2	–	–	2496.96 ± 101.55^{a}	63.01 ± 0.77^{c}	1052.26 ± 42.14^{c}	35.79 ± 2.01^{b}	14.04 ± 0.93^{b}
	3	–	–	1014.80 ± 74.63^{d}	72.81 ± 1.02^{b}	1637.37 ± 75.73^{a}	35.64 ± 1.71^{b}	17.08 ± 0.97^{a}
	4	–	–	1411.77 ± 62.35^{c}	77.51 ± 0.84^{a}	1512.80 ± 65.77^{b}	54.48 ± 2.46^{a}	19.03 ± 0.80^{a}
Simulated eutrophication	E0	8.35 ± 5.75^{a}	14.44 ± 3.66^{d}	1781.53 ± 107.88^{a}	68.22 ± 1.42^{ab}	1309.00 ± 135.17^{a}	25.51 ± 2.11^{c}	12.40 ± 0.76^{c}
	E1	0.41 ± 5.12^{a}	17.77 ± 1.68^{b}	1930.69 ± 129.74^{a}	66.29 ± 1.63^{ab}	1263.42 ± 92.18^{a}	36.43 ± 3.00^{b}	12.64 ± 0.74^{c}
	E2	-17.82 ± 3.29^{b}	16.45 ± 3.20^{c}	1763.27 ± 128.20^{a}	70.66 ± 1.61^{a}	1105.88 ± 73.13^{ab}	38.50 ± 2.28^{ab}	15.90 ± 0.79^{b}
	E3	-20.42 ± 2.84^{b}	19.72 ± 1.04^{a}	1310.06 ± 97.78^{b}	65.50 ± 1.96^{b}	919.84 ± 64.81^{b}	45.23 ± 2.73^{a}	20.72 ± 0.97^{a}
SAR	pH 7.0	0.21 ± 4.96^{a}	19.14 ± 1.24^{a}	2026.03 ± 104.79^{a}	67.86 ± 1.26^{ab}	1274.07 ± 99.30^{a}	30.33 ± 2.46^{b}	11.63 ± 0.49^{c}
	pH 5.0	-4.22 ± 5.16^{a}	17.06 ± 1.81^{b}	1617.74 ± 98.82^{b}	69.91 ± 1.34^{a}	1182.46 ± 84.78^{ab}	37.95 ± 2.38^{a}	15.11 ± 0.92^{b}
	pH 4.0	-18.10 ± 3.84^{b}	15.09 ± 4.29^{c}	1445.39 ± 96.62^{b}	65.16 ± 1.68^{b}	992.08 ± 61.97^{b}	40.98 ± 2.19^{a}	19.51 ± 0.70^{a}

Results are expressed as mean of triplicate samples ± standard error. Different lowercase letters in the same column of a main effect indicate significant differences at $P < 0.05$

E1 ($P=0.588$), but significant decreases were detected in E2 and E3 ($P<0.05$) (Table 4). This result indicated that mild eutrophication (E1) had no discernible inhibitory effects on plant biomass. Under various main effects of SAR, the RGR showed significant variances (Table 3). The RGR significantly decreased as the SAR concentration increased ($P<0.05$), indicating that SAR spraying inhibited *P. cordata* growth.

Root activity

Under the main effects of simulated eutrophication or SAR, significant variations in the root activity of *P. cordata* were found (Table 3). As the eutrophication level and SAR concentration increased, significant increases and decreases in the root activity of *P. cordata* were observed, respectively ($P<0.05$) (Table 4). The root activity under different interactive effects of eutrophication and SAR presented the significant differences ($F=807.998$, $df=11/35$, $P<0.05$; Fig. 1a). Compared to the control, significant increases in the root activity under compound stress only occurred in E1 + pH 7.0 ($P<0.05$), which reached the highest value of 16.31 $\mu g \cdot g^{-1} \cdot h^{-1}$. In E0, E1, and E2, SAR application led to significant decreases in root activity when compared to the control. In E3, no significant differences in root activity were detected under the SAR treatment.

Chl T content

The Chl *T* content of *P. cordata* leaves under different main effects of simulated eutrophication showed the significant differences (Table 3). Compared to the control, no significant differences were detected in the Chl *T* content of *P. cordata* leaves in E1 and E2, but the Chl *T* content significantly decreased by 26.46% in E3 ($P<0.05$). Significant variations in the Chl *T* content under different main effects of SAR were observed (Table 3). SAR (pH = 5.0 and 4.0) treatment led to a significant decrease in the Chl *T* content when compared to the control ($P<0.05$). Significant differences were detected in the Chl *T* content under different main effects of SAR spraying time (Table 3). As the SAR spraying time increased, the Chl *T* content in the leaves increased at first and then decreased (Table 4). The Chl *T* content underwent significant changes as a result of various interactions effects of eutrophication and SAR for 28 d ($F=70.444$, $df=11/35$, $P<0.05$; Fig. 1b). When sprayed with SAR for 28 d, the plants exposed to eutrophication exhibited reductions in the Chl *T* content when compared to the control. The Chl *T* content in E3 + pH 4.0 reached the lowest value (769.81 $mg \cdot g^{-1}$), which was significantly lower than the control by 63.21% ($P<0.05$).

SOD activity

Compared to the control, eutrophication and SAR exerted no obvious inhibitory effects on the SOD activity of *P. cordata* (Table 4). Significant differences were observed in the SOD activity under different main effects of SAR spraying time (Table 3). As SAR spraying time increased, the SOD activity in the leaves exhibited a significant upward trend ($P<0.05$) (Table 4). Under various interactive effects of eutrophication and SAR for 28 d, significant variations in the SOD activity were identified ($F=309.917$, $df=11/35$, $P<0.05$; Fig. 1c). SAR treatment in plants exposed to eutrophication for 28 d resulted in a significant decrease in the SOD activity when compared to the control (87.21 $U \cdot g^{-1}$), which was similar to the Chl *T* content results. Additionally, as the eutrophication level increased, the SOD activity in the control exhibited a decreasing trend at first and then increased, while the pH 4.0 group increased at first and then decreased ($P<0.05$). Moreover, when compared to the control, the SOD activities of plants in E1, E2, and E3 that were treated with SAR pH 4.0 were significantly higher than those treated with SAR pH 7.0 and 5.0 ($P<0.05$).

CAT activity

Significant differences were identified in the CAT activity of *P. cordata* under different main effects of simulated eutrophication (Table 3). Compared to the control, no significant differences were detected in the CAT activity of *P. cordata* in E1 and E2, but the CAT activity significantly decreased by 29.73% in E3. Under various primary SAR effects, there were discernible changes in the CAT activity (Table 3). No significant differences were detected in the CAT activity between the SAR pH 5.0 and 7.0 treatments, while SAR pH 4.0 significantly decreased the CAT activity by 22.13% ($P<0.05$). Significant variations in the CAT activity were found under several main effects of SAR spraying time (Table 3). As SAR spraying time increased, the CAT activity increased at first and then decreased, reaching the highest value at the third spraying time (Table 4). Significant differences were detected in the CAT activity under different interactive effects of eutrophication and SAR for 28 d ($F=55.807$, $df=11/35$, $P<0.05$; Fig. 1d). The highest CAT activity value (2500.16 $U \cdot g^{-1} \cdot min^{-1}$) was detected in the control ($P<0.05$). In E0, E2, and E3, the CAT activity in plants treated with SAR pH 4.0 significantly decreased by 22.51%, 29.98%, and 22.55%, respectively, when compared to that in plants treated with SAR pH 5.0 ($P<0.05$). In E1, SAR treatment had no significant inhibitory effect on the CAT activity.

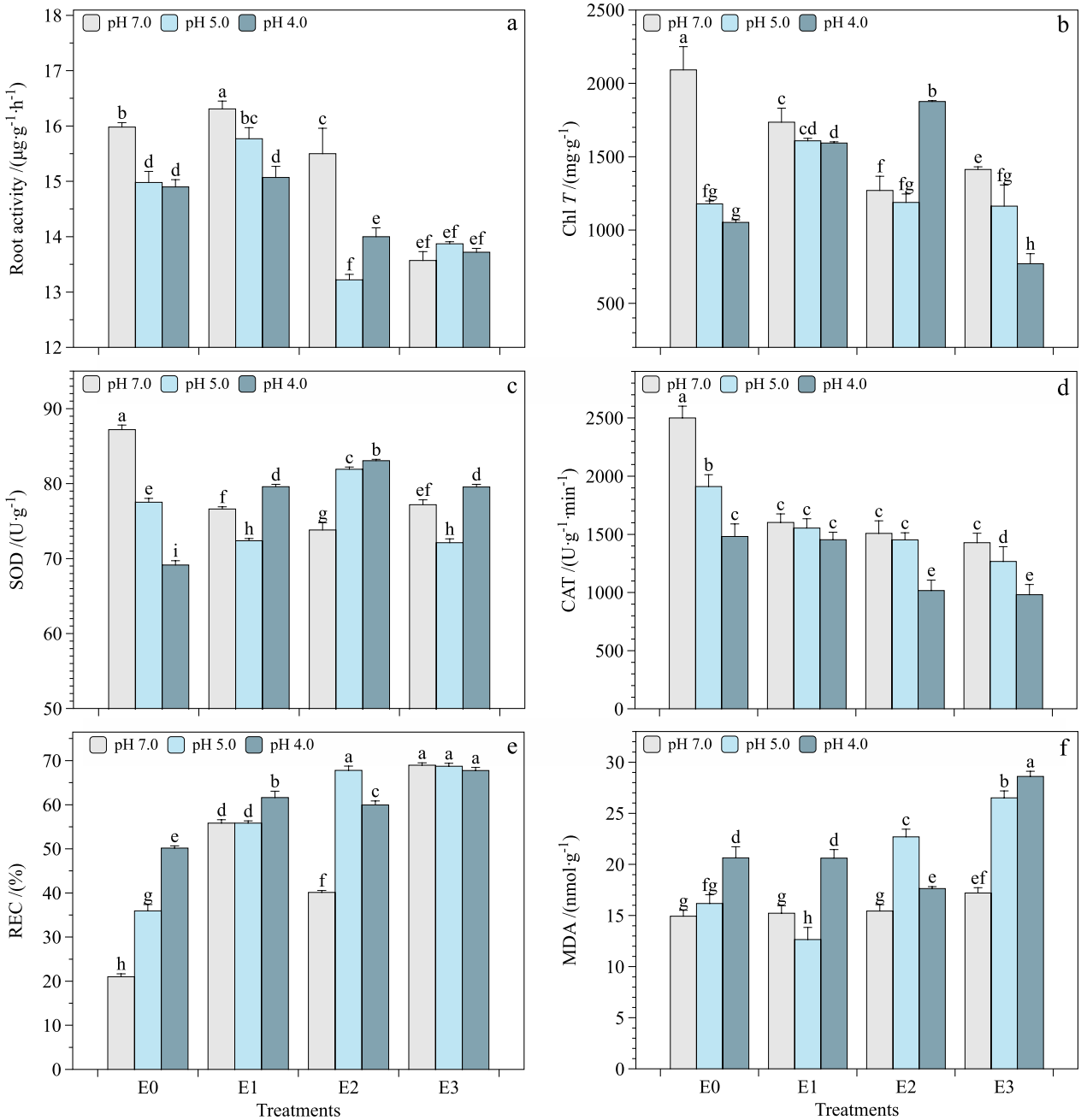

Fig. 1 The interactive effects of simulated eutrophication and simulated acid rain (SAR) on the root activity (**a**), Chl *T* (**b**), SOD (**c**), CAT (**d**), REC (**e**), and MDA (f) of *P. cordata* harvested on day 28. Results are expressed as mean of triplicate samples ± standard error. Different lowercase letters indicate significant differences at $P < 0.05$

Relative conductivity (REC)

Under various main effects of simulated eutrophication, SAR, or SAR spraying time, significant changes were seen in the REC of *P. cordata* (Table 3). As the eutrophication level, SAR concentration, and SAR spraying time increased, the REC in *P. cordata* leaves significantly increased ($P < 0.05$) (Table 4). Significant differences were found in the REC under different interactive effects of eutrophication and SAR for 28 d ($F = 942.548$, $df = 11/35$, $P < 0.05$; Fig. 1e). In E0 and E1, the REC in the leaves treated with SAR pH 4.0 for 28 d was significantly higher than that in the leaves treated with SAR pH 7.0 and 5.0. In E2, the REC reached the highest value (67.80%) under SAR pH 5.0. In E3, the REC values of the three SAR

treatments significantly increased, which were 3.28, 3.27, and 3.23 times higher than that of the control ($P<0.05$).

MDA content

The MDA content of *P. cordata* under different main effects of simulated eutrophication or SAR showed significant variations (Table 3). The change trends of the MDA contents of plants under compound stress were the same as REC and reached the highest value in E3 under SAR pH 4.0 treatment. Significant differences were identified in the CAT activity under different main effects of SAR spraying time (Table 3). As SAR spraying time increased, the change in the MDA content was similar to REC, showing a significant upward trend ($P<0.05$) (Table 4). Under various interactive effects of eutrophication and SAR for 28 d, significant variations in the MDA content were found ($F=126.764$, $df=11/35$, $P<0.05$; Fig. 1f). Compared to the control, the MDA content of plants treated with SAR pH 4.0 for 28 d and exposed to different levels of eutrophication significantly increased by 18.15–91.63% ($P<0.05$). In E2 and E3, the MDA content of plants treated with SAR pH 5.0 and 4.0 was significantly higher than that of plants treated with SAR pH 7.0 ($P<0.05$). E3 + pH 4.0 had the highest MDA content (28.62 nmol·g^{-1}).

Effects of simulated eutrophication and acid rain compound stress on *P. cordata* algae inhibition

Inhibition rate of M. aeruginosa

The inhibition rate on algae of various cultured water samples presented the significant differences ($F=30.936$, $df=11/71$, $P<0.05$; Fig. 2). The inhibition rate on *M. aeruginosa* of the control reached the highest value (42.11%), which indicated that the inhibition effects on algal growth of cultured water samples from plants under compound stress were significantly reduced ($P<0.05$). In E1, E2, and E3, significant differences were detected between the algal inhibition rates of cultured water samples from plants treated with SAR pH 5.0 and 4.0 ($P<0.05$). Among these, E2 and E3 exhibited significant decreases in the algal inhibition rate when compared to pH 7.0 ($P<0.05$). Additionally, under the same SAR concentration, the algae inhibition rates of cultured water samples significantly decreased as the eutrophication level increased ($P<0.05$).

Chl a content of algal cells

Significant differences were detected in the Chl *a* content of algae cells under different main effects of processing time or cultured water sample ($F=27.307$, $df=3/287$, $P<0.05$; $F=20.461$, $d.f=11/287$, $P<0.05$; Table 5). Over time, the Chl *a* content of algae cells significantly decreased at first and then increased, reaching the lowest and highest values on days 5 and 7, respectively ($P<0.05$). In E0 and E3, the Chl *a* content significantly increased as the SAR concentration increased, reaching the highest value in E0 + pH 4.0. In E1 and E2, the Chl *a* content exhibited the opposite trend, reaching the lowest value in E2 + pH 4.0 ($P<0.05$). On day 1, the Chl *a* content significantly increased by 13.60–17.48% in E0 + pH 4.0, E1 + pH 7.0, E1 + pH 5.0, and E2 + pH 7.0 when compared to the control, but significantly decreased by 12.61–22.31% in E2 + pH 5.0, E2 + pH 4.0, and E3 + pH 7.0 (Fig. 3a). On day 3, the Chl *a* content in E0 + pH 5.0, E0 + pH 4.0, and E3 + pH 4.0 significantly increased when compared to the control. On days 5 and 7, the Chl *a* content in E0 + pH 5.0, E0 + pH 4.0, and E3 + pH 4.0 exhibited the same change trends ($P<0.05$).

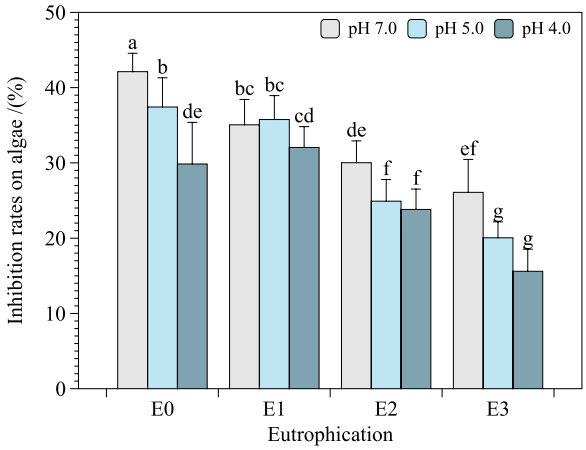

Fig. 2 Various cultured water samples from *P. cordata* under compound stress on the inhibition rate of *M. aeruginosa*. Results are expressed as mean of triplicate samples ± standard error. Different lowercase letters indicate significant differences at $P<0.05$

SOD activity of algal cells

The SOD activity of algal cells under different main effects of processing time or cultured water sample showed significant differences ($F=13.043$, $df=3/287$, $P<0.05$; $F=7.949$, $d.f=11/287$, $P<0.05$; Table 5). The SOD activity of algae cells in cultured water samples of *P. cordata* reached the highest value on day 7, and its change trend was similar to the Chl *a* content. Compared to the control, the cultured water samples of *P. cordata* under compound stress exerted significant inhibitory effects on the SOD activity of algae cells ($P<0.05$). Compared to E2, the SOD activity of algae cells in E0, E1, and E3 significantly decreased as the SAR concentration increased, reaching the lowest value in E3 + pH 4.0 ($P<0.05$). On day 1, the SOD activities of algae cells in E0 + pH 5.0, E0 + pH 4.0, and E1 + pH 7.0 were not significantly different when

Table 5 The main effects of processing time or cultured water sample on *Microcystis aeruginosa*

Main effects		Index		
		Chl *a* content ($\mu g \cdot L^{-1}$)	SOD activities ($U \cdot mL^{-1}$)	MDA content ($\mu mol \cdot L^{-1} \cdot FW$)
Processing time (d)	1	0.37 ± 0.06^{b}	2.64 ± 0.11^{c}	0.45 ± 0.18^{b}
	3	0.33 ± 0.06^{c}	2.56 ± 0.11^{d}	0.52 ± 0.13^{a}
	5	0.30 ± 0.10^{d}	2.66 ± 0.13^{b}	0.31 ± 0.07^{c}
	7	0.41 ± 0.08^{a}	2.67 ± 0.12^{a}	0.26 ± 0.15^{d}
Cultured water sample	E0 + pH 7.0	0.33 ± 0.05^{ef}	2.78 ± 0.15^{a}	0.40 ± 0.17^{abcd}
	E0 + pH 5.0	0.41 ± 0.06^{c}	2.67 ± 0.14^{c}	0.37 ± 0.19^{cd}
	E0 + pH 4.0	0.44 ± 0.06^{a}	2.63 ± 0.15^{de}	0.36 ± 0.14^{d}
	E1 + pH 7.0	0.38 ± 0.06^{d}	2.64 ± 0.10^{d}	0.39 ± 0.21^{abcd}
	E1 + pH 5.0	0.34 ± 0.07^{e}	2.62 ± 0.10^{fg}	0.41 ± 0.15^{ab}
	E1 + pH 4.0	0.28 ± 0.06^{h}	2.61 ± 0.07^{g}	0.37 ± 0.15^{d}
	E2 + pH 7.0	0.38 ± 0.04^{d}	2.62 ± 0.08^{ef}	0.38 ± 0.17^{bcd}
	E2 + pH 5.0	0.30 ± 0.06^{g}	2.64 ± 0.07^{d}	0.38 ± 0.19^{bcd}
	E2 + pH 4.0	0.24 ± 0.08^{i}	2.64 ± 0.12^{d}	0.42 ± 0.21^{a}
	E3 + pH 7.0	0.33 ± 0.08^{f}	2.69 ± 0.09^{b}	0.37 ± 0.12^{cd}
	E3 + pH 5.0	0.38 ± 0.06^{d}	2.58 ± 0.11^{h}	0.38 ± 0.16^{bcd}
	E3 + pH 4.0	0.42 ± 0.07^{b}	2.51 ± 0.11^{i}	0.40 ± 0.23^{abc}

Results are expressed as mean of triplicate samples ± standard error. Different lowercase letters in the same column of a main effect indicate significant differences at $P < 0.05$

compared to the control, while the SOD activities of other water samples significantly decreased ($P < 0.05$) (Fig. 3b). On days 3, 5, and 7, the highest SOD activity was detected in E0 + pH 7.0 ($P < 0.05$).

MDA content of algal cells

Under the main effects of processing time, there were significant changes found in the MDA content of algal cells ($F = 54.412$, $df = 3/287$, $P < 0.05$; Table 5). Over time, the MDA content of algal cells exhibited the opposite trend as the SOD activity, reaching the highest and lowest values on days 3 and 7, respectively ($P < 0.05$). Under compound stress, no significant differences were detected in the MDA content of algal cells when compared to the control ($F = 0.218$, $df = 11/287$, $P = 0.996$; Table 5). On day 1, when compared to the control, the MDA contents in E0 + pH 5.0 and E2 + pH 7.0 significantly increased by 12.5% and 2.5%, respectively ($P < 0.05$), while no significant differences were detected in other water samples (Fig. 3c). On days 3 and 5, the highest MDA content of algal cells appeared in E0 + pH 7.0 and E3 + pH 4.0. On day 7, when compared to the control, the MDA content in the six water samples from E1 and E2 significantly increased but significantly decreased in E0 + pH 4.0 and E3 + pH 4.0 ($P < 0.05$).

Discussion

Chlorophyll, a photosynthetic pigment, serves as the building block for capturing light energy in plant leaves, and the amount of it reflects a plant's capacity for photosynthesis. In this experiment, under mild (E1) and moderate (E2) eutrophication, no significant change was detected in the Chl *T* content of *P. cordata* leaves when compared to the control (E0) (Table 4). This result indicated that *P. cordata* absorbs N and P elements normally and consistently within a range of nutrient concentrations, ensuring the biosynthesis of chlorophyll in the leaves. Excessive concentrations of N and P prevented chlorophyll synthesis or accelerated its decomposition (Table 4), resulting in limited photosynthesis and biomass growth. Additionally, the Chl *T* content in the leaves significantly decreased under SAR pH 5.0 and 4.0 (Table 4), which was consistent with a previous study on two tomato cultivars (Debnath et al. 2018). This might be as a result of H^+ accumulating in plant tissues and taking the place of Mg^{2+} in the chlorophyll molecules, thereby reducing the chlorophyll content by converting chlorophyll into pheophytin (Eguagie et al. 2016; Pham et al. 2021). The degree of plant damage can be directly characterized by changes in biomass when the plant is under stress. Similar to the research done by Pham et al. (2021) on soybean (*Glycine max*), plant biomass decreased as the SAR pH value rose. Therefore, we speculated that

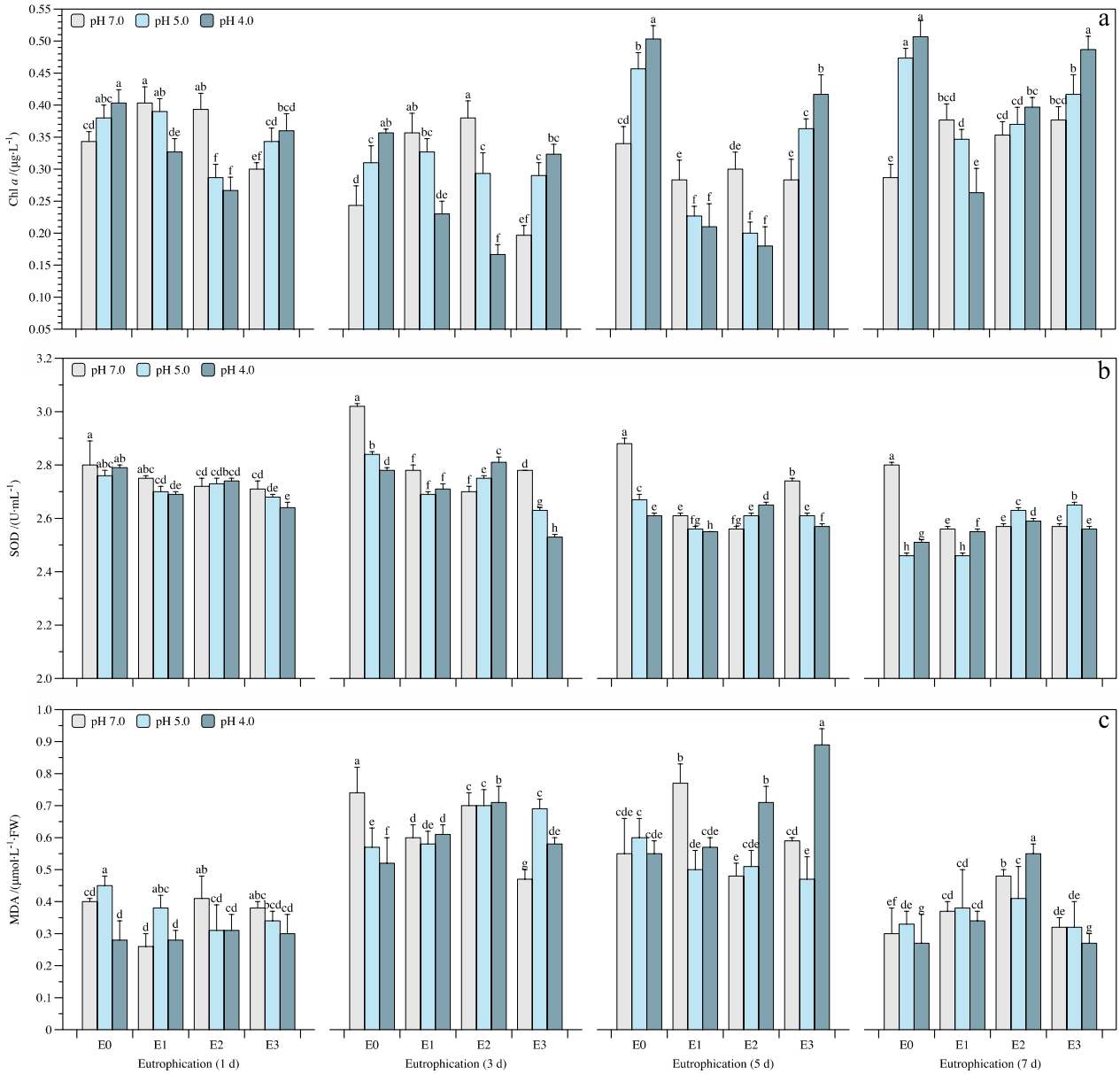

Fig. 3 Variations in the Chl *a* (**a**), SOD (**b**), and CAT (**c**) of *M. aeruginosa* cells in various cultured water samples from *P. cordata* under compound stress for 1, 3, 5, and 7 d, respectively. Results are expressed as mean of triplicate samples ± standard error. Different lowercase letters indicate significant differences at $P < 0.05$

SAR decreased H^+-ATPase activity in the plasma membrane of *P. cordata*, impeded the transmembrane chemical gradient of H^+, and consequently prevented the electrical gradient. That ultimately destroyed the energy source of plant growth, and thereby inhibited the accumulation of biomass (Falhof et al. 2016).

Reactive oxygen species (ROS), such as the superoxide anion (O_2^-), hydrogen peroxide (H_2O_2), hydroxyl radical (HO), and singlet oxygen ($^1O_2$), can build up excessively in response to stress. This interfered with the normal physiological metabolism of plants by increasing membrane permeability, causing lipid peroxidation of the cell membrane, and allowing some nutrient ions to exosmose through the membrane. The MDA is the final product of plant cell membrane lipid peroxidation and the REC is a crucial index for assessing the stability and integrity of plant cell membranes. In this study, SAR pH 4.0 and E3 + pH 4.0 both resulted in significantly increased REC and MDA content in *P. cordata* leaves (Fig. 1; Table 4). These results may be explained by the

following: (1) strong acid rain directly raised the extracellular H^+ concentration, which led to higher H^+ concentrations inside of cells. This imbalanced the metabolism of ROS by increasing the production of ROS relative to its clearance. (2) Elevated cytosol protons under strong acidic conditions caused Ca^{2+} to be lost from the cell membrane through replacement, which compromised the stability of the membrane system. (3) Strong acid rain stress enhanced the acid phosphatase activity of *P. cordata* leaves, promoted the degreasing reaction of the phospholipid bilayer in the membrane, and destroyed the membrane system's integrity (Ren et al. 2018). The SOD acts as the first line of defense against oxidation and catalyzes the disproportionation of O_2^- to generate H_2O_2 and O_2, while CAT catalyzes the rapid decomposition of H_2O_2 into H_2O and O_2 (Bezerril Fontenele et al. 2017). The synergistic effects of SOD and CAT lessen the buildup of oxygen free radicals and prevent the conversion of O_2^- and H_2O_2 into highly destructive HO molecule via the Haber–Weiss and Fenton reactions. As a result, free radical damage to biological macromolecules like nucleic acids, proteins (enzymes), and biofilms is avoided or reduced. In this study, the MDA content and SOD and CAT activities of *P. cordata* leaves did not differ from the control when mild eutrophication was present (Table 4). That indicated the plants maintained the antioxidant capacity by stabilizing the SOD and CAT activities, which is an ecological response strategy used by *P. cordata* to adapt to mild eutrophication. Severe (E3) eutrophication, strong acid rain, and compound stress all led to inhibited SOD and CAT activities, intensified oxidative damage, and inhibited metabolic activities, as evidenced by increased REC and MDA contents, as well as diminished allelopathic algal inhibition effects in the leaves (Fig. 2).

Allelopathy is an environmental adaptation mechanism produced by plants to enhance their competitiveness and survival during evolution. Allelochemicals released by macrophytes directly inhibit the growth of adjacent phytoplankton in terms of cell density, providing conclusive evidence of allelopathy (Fernandez et al. 2016; Nakai et al. 1999). According to Tian et al. (2011), the cultured water of *P. cordata* exerted a strong inhibitory effect on *M. aeruginosa* under normal growth conditions. In this study, under mild eutrophication, SAR had no discernible inhibitory effects on the allelopathic algal inhibition ability of *P. cordata*, which remained a high level. Under moderate and severe eutrophication, SAR was the main reason for the reduced allelopathic algal inhibition capacity (Fig. 3). According to the GDBH (Bauer et al. 2010), *P. cordata* allocates more of its limited life resources to self-repair processes in order to withstand oxidative stress under the compound stress of moderate or severe eutrophication and acid rain. That revealed this plant modifies its resource inputs of allelochemicals in response to changes in the growth environment. Previous studies reported that active allelopathic components, such as flavonoids, tannins, ρ-coumaric acid, and vanillic acid, released by aquatic plants significantly decreased the Chl *a* content in *M. aeruginosa* cells (Tazart et al. 2019; Zhang et al. 2010). This was in line with the results of this study, which indicated that the *P. cordata* allelochemicals in cultured water samples interfered with the photosynthesis of algae cells by inhibiting the Chl *a* content. That was one mechanism through which *P. cordata* inhibited *M. aeruginosa* growth. Additionally, algal cells' SOD activity was low and their MDA content was high on days 1 and 3 (Table 5), demonstrating that the oxidative stress induced by the allelochemicals released by *P. cordata* under compound stress may lead to: (1) leakage of Cu, Zn, Fe, and other metal ions from algal cells, which inhibited the antioxidant enzyme activity of algal cells (Zuo et al. 2016); or (2) leakage of cell components, such as proteins, nucleic acids, and inorganic ions, the enhancement of proton influx, increased cell membrane permeability, and damage to the cell membrane (Campos et al. 2009). On day 7, the Chl *a* content and SOD activity of algal cells significantly increased (Table 5). Zuo et al. (2016) discovered that allelochemicals easily degrade, in light of the fact that allelopathy effectiveness necessitates the continuous and stable release of allelochemicals. Therefore, we speculated that *P. cordata* allelochemicals at low concentrations caused by degradation exerted hormesis effects on the Chl *a* content and SOD activity of *M. aeruginosa* at this time (Calabreseci 1999).

Conclusions

Under mild eutrophication (E1, 2 $mg{\cdot}L^{-1}$ TN, 0.4 $mg{\cdot}L^{-1}$ TP, and 15 $mg{\cdot}L^{-1}$ COD_{Mn}), *P. cordata* grew normally. Under compound stress of mild eutrophication (E1) and SAR (pH = 4 and pH = 5), cultured water samples of *P. cordata* maintained strong algal inhibitory effects in terms of reduced Chl *a* content and SOD activity. The compound eutrophication and SAR stress decreased the Chl *T* content and SOD and CAT activities in *P. cordata*, giving rise to oxidative damage. Under moderate (E2) and severe (E3) eutrophication, the SAR accounted for the reduced allelopathic algal inhibition capacity of the plants. Generally, *P. cordata* possesses essential landscape effects and ecological benefits in mildly eutrophic waters of areas afflicted with acid rain.

Abbreviations

TN	Total nitrogen
TP	Total phosphorus
SAR	Simulated acid rain

SOD	Superoxide dismutase
CAT	Catalase
ATP	Adenosine triphosphate
GDBH	Growth–differentiation balance hypothesis
RGR	Relative growth rate
Chl *T*	Total chlorophyll
REC	Relative conductivity
MDA	Malondialdehyde
TBA	Thiobarbituric acid
IR	Inhibition rates
NBT	Nitrogen blue tetrazole
ROS	Reactive oxygen species
O_2^-	Superoxide anion
H_2O_2	Hydrogen peroxide
HO	Hydroxyl radical
$^1O_2$	Singlet oxygen

Supplementary Information

The online version contains supplementary material available at https://doi.org/10.1186/s13717-023-00467-4.

Additional file 1. The raw data of the RGR, root activity, Chl T content, SOD activity, CAT activity, REC, and MDA content of *P. cordata* under the simulated acid rain spraying times, simulated acid rain and simulated eutrophication.

Acknowledgements
We would like to thank LetPub (www.letpub.com) for its linguistic assistance during the preparation of this manuscript.

Author contributions
YL contributed significantly to the data analyses and the original manuscript. XQ performed the experiment. JX and CZ contributed to the investigation, manuscript preparation and formal analysis. RT contributed to the conception, supervision and funding assistant of the study. All authors read and approved the final manuscript.

Funding
This study was financially supported by the National Natural Science Foundation of China (No. 31670698), the Project Funded by China Postdoctoral Science Foundation (No. 2020M671509), and the Postgraduate Research & Practice Innovation Program of Jiangsu Province (No. KYCX23_1255).

Availability of data and materials
The datasets used and analyzed during the current study are available from the corresponding author on reasonable request.

Declarations

Ethics approval and consent to participate
Not applicable.

Consent for publication
Not applicable.

Competing interests
The authors declare that they have no competing interests.

Received: 6 January 2023 Accepted: 3 November 2023
Published online: 28 November 2023

References

Allen JL, Ten-Hage L, Leflaive J (2017) Regulation of fatty acid production and release in benthic algae: could parallel allelopathy be explained with plant defence theories? Microb Ecol 75(3):609–621
Andrade GC, Letícia NC, Silva L (2020) Micromorphological alterations induced by simulated acid rain on the leaf surface of *Joannesia princeps* Vell. (Euphorbiaceae). Ecol Indic 116:106526
Bauer N, Blaschke U, Beutler E et al (2010) Seasonal and interannual dynamics of polyphenols in *Myriophyllum verticillatum* and their allelopathic activity on *Anabaena variabilis*. Aquat Bot 91:110–116
BezerrilFontenele NM, Oliveira Otoch ML, Gomes-Rochette NF et al (2017) Effect of lead on physiological and antioxidant responses in two *Vigna unguiculata* cultivars differing in Pb-accumulation. Chemosphere 176:397–404
Calabreseci EJ (1999) Evidence that hormesis represents an "overcompensation" response to a disruption in homeostasis. Ecotoxicol Environ Saf 42(2):135–137
Campos FM, Couto JA, Figueiredo AR et al (2009) Cell membrane damage induced by phenolic acids on wine lactic acid bacteria. Int J Food Microbiol 135:144–151
Chen YW, Chen KN, Hu YH (2006) Discussion on possible error for phytoplankton chlorophyll-*a* concentration analysis using hot-ethanol extraction method. J Lake Sci 18(5):550–552
Chen MM (2018) Bulletin on environmental conditions of Jiangsu Province in 2017. Xinhua Daily, Nanjing
D'Anglada LV (2021) Public health surveillance, public communication and participation. In: Toxic Cyanobacteria in Water, pp 801–828
Debnath B, Irshad M, Mitra S et al (2018) Acid rain deposition modulates photosynthesis, enzymatic and non-enzymatic antioxidant activities in tomato. Int J Environ Res 12:203–214
Du J, Qv W, Niu Y et al (2022) Co-exposures of acid rain and ZnO nanoparticles accelerate decomposition of aquatic leaf litter. J Hazard Mater 426:128141
Eguagie MO, Aiwansoba RP, Omofomwan KO et al (2016) Impact of simulated acid rain on the growth, yield and plant component of *Abelmoschus caillei*. J Adv Biol Biotechnol 6:1–6
Falhof J, Pedersen JT, Fuglsang AT et al (2016) Plasma membrane H^+-ATPase regulation in the center of plant physiology. Mol Plant 9(3):323–337
Fernandez C, Monnier Y, Santonja M et al (2016) The impact of competition and allelopathy on the trade-off between plant defense and growth in two contrasting tree species. Front Plant Sci 7:594
Gao JF (2006) Experimental guidance of plant physiology. Higher Education Press, Beijing
Hilt S, Gross EM (2008) Can allelopathically active submerged macrophytes stabilise clear-water states in shallow lakes. Basic Appl Ecol 9:422–432
Ho JC, Michalak AM, Pahlevan N (2019) Widespread global increase in intense lake phytoplankton blooms since the 1980s. Nature 574(7780):667–670
Huisman J, Codd GA, Paerl HW et al (2018) Cyanobacterial blooms. Nat Rev Microbiol 16:471–483
Kong Y, Peng Y, Zhang Z et al (2019) Removal of *Microcystis aeruginosa* by ultrasound: inactivation mechanism and release of algal organic matter. Ultrason Sonochem 56:447–457
Lee J, Kumar P, Jae Y et al (2017) The role of algae and cyanobacteria in the production and release of odorants in water. Environ Pollut 227:252–262
Li QY, Liu X, Zhang JC (2021) Changing trends of acid rain types in the Yangtze River Delta region. J Nanjing For Univ 45(1):168–174
Ministry of Environmental Protection of the People's Republic of China (2002) Surface water environment quality standard (GB 3838-2002). China Environmental Science Press, Beijing
Mjelde M, Faafeng B (1997) *Ceratophyllum demersum* hampers phytoplankton development in some small Norwegian lakes over a wide range of phosphorus level and geographic latitude. Freshw Biol 37:355–365
Nakai S, Inoue Y, Hosomi M et al (1999) Growth inhibition of blue-green algae by allelopathic effects of macrophytes. Water Sci Technol 39:47–53
Neves NR, Oliva MA, Centeno D et al (2009) Photosynthesis and oxidative stress in the restinga plant species *Eugenia uniflora* L. exposed to simulated acid rain and iron ore dust deposition: potential use in environmental risk assessment. Sci Total Environ 407(12):3740–3745

Pham H, Nguyen AT, Do A et al (2021) Impacts of simulated acid rain on the growth and the yield of soybean (*Glycine max* (L.) Merr.) in the mountains of Northern Vietnam. Sustainability 13(9):4980
Princiotta SD, Hendricks SP, White DS (2019) Production of cyanotoxins by *Microcystis aeruginosa* mediates interactions with the mixotrophic flagellate cryptomonas. Toxins 11(4):223
Qian YP, Li XT, Tian RN (2019) Effects of aqueous extracts from the rhizome of *Pontederia cordata* on the growth and interspecific competition of two algal species. Ecotoxicol Environ Saf 168:401–407
Ren XQ, Zhu JZ, Liu HY et al (2018) Response of antioxidative system in rice (*Oryza sativa*) leaves to simulated acid rain stress. Ecotoxicol Environ Saf 148:851–856
Tazart Z, Douma M, Tebaa L et al (2019) Use of macrophytes allelopathy in the biocontrol of harmful *Microcystis aeruginosa* blooms. Water Supply 19(1):245–253
Tazart Z, Manganelli M, Scardala S et al (2021) Remediation strategies to control toxic cyanobacterial blooms: effects of macrophyte aqueous extracts on *Microcystis aeruginosa* (growth, toxin production and oxidative stress response) and on bacterial ectoenzymatic activities. Microorganisms 9(8):1782
Tian RN, Sun XX, Wei Y et al (2011) Effects of hydrophytes on the growth of *Microcystis aeruginosa*, *Scenedesmus obliqnus* and *Chlorella vulgaris*. Chin J Ecol 30(12):2732–2738
Verónica M, Rodríguez S, Rosas U et al (2020) Does acid rain alter the leaf anatomy and photosynthetic pigments in urban trees? Plants 9(7):862
Visser PM, Ibelings BW, Bormans M et al (2016) Artificial mixing to control cyanobacterial blooms: a review. Aquat Ecol 50(3):423–441
Wang XK (2006) Principles and techniques of plant physiological and biochemical experiments. Higher Education Press, Beijing
Wang Z, Chen Y, Xie P et al (2016a) Removal of *Microcystis aeruginosa* by UV-activated persulfate: performance and characteristics. Chem Eng J 300:245–253
Wang R, Hua M, Yu Y et al (2016b) Evaluating of effects of allelochemical ferulic acid on *Microcystis aeruginosa* by pulse-amplitude-modulated (PAM) fluorometry and flow cytometry. Chemosphere 147:264–271
Wang X, Zha Y, Jiang X et al (2018) The growth and physiological activity of *Microcystis aeruginosa* after flocculation using modified tannin. Int Biodeterior Biodegr 133:180–186
Wu YB, Ye B (2016) Effects of combined elevated temperature and drought stress on anti-oxidative enzyme activities and reactive oxygen species metabolism of *Broussonetia papyrifera* seedlings. Acta Ecol Sin 36(2):403–410
Zhang TT, Zheng CY, Wei H et al (2010) The allelopathy and allelopathic mechanism of phenolic acids on toxic *Microcystis aeruginosa*. J Appl Phycol 22(1):71–77
Zuo SP, Zhou SB, Ye LT et al (2016) Synergistic and antagonistic interactions among five allelochemicals with antialgal effects on bloom-forming *Microcystis aeruginosa*. Ecol Eng 97:486–492

Publisher's Note